Nuclear Instruments and Methods in Physics Research A300 (1991) 480–492
North-Holland

Test of a prototype of the ZEUS backing calorimeter

I. Kudla, R.J. Nowak, R. Walczak and A.F. Zarnecki
*Institute of Experimental Physics, Warsaw University *, Poland*

H. Abramowicz **
Deutsches Elektronen-Synchrotron DESY, Hamburg, Germany

Received 30 August 1990

We have studied the performance of a high resolution uranium–scintillator calorimeter followed by a much coarser backing calorimeter, made out of iron plates interleaved with planes of limited streamer tubes. The test results, obtained at the CERN-SPS hadron beam, show that the backing calorimeter can be used either to veto events with significant energy leakage from the uranium calorimeter or to correct for the energy. In both cases the energy resolution of the combined calorimeters improves significantly compared to the uranium calorimeter alone.

1. Introduction

The forthcoming new high energy accelerator facilities have revived the interest in studying new solutions for calorimetric energy measurements. An interesting solution for optimizing energy measurements in terms of resolution and cost has been put forward by two experiments ZEUS [1] and H1 [2], aiming to study high energy ep scattering at the electron–proton storage ring HERA, currently being built at Hamburg-DESY. The external iron yoke and muon absorber, surrounding the main components of the detector, is to be instrumented in such a way as to allow a complementary energy measurement for showers leaking out of the central, high resolution calorimeter.

In case of the ZEUS experiment, the main calorimeter is to be a sampling calorimeter made of depleted uranium (DU for short) and scintillator. As part of the preparation for the experiment, a test was built, consisting of a uranium calorimeter $7\lambda_{int}$ long, made out of 3.2 mm DU and 3 mm scintillator plates, followed by an iron backing calorimeter made out of ten 5 cm thick Fe plates interleaved with limited streamer tubes as active material. This setup has been exposed to the X-5 test beam at the CERN SPS, where the beam momentum could be varied between 5 and 100 GeV/c. The results on the performance of the stand-alone DU calorimeter have been presented elsewhere [3]. In this paper we would like to concentrate on results obtained for the iron calorimeter, as a stand-alone unit and as a backing device.

* Partly supported by CPBP 01.06 and 01.09.

** Alexander von Humboldt Fellow, on leave of absence from Institute of Experimental Physics, Warsaw University, Poland.

2. Experimental setup

2.1. Beam

The X-5 test beam at the CERN SPS provides hadron, muon and electron beams with momenta ranging from 5 to 100 GeV. The particle composition depends on the beam momentum and the target material and thickness used in this secondary beam. An enhancement of the electron content of the beam can be obtained up to 50 GeV by means of lead foils that serve as a convertor for photons originating from π^0 decay. Two 10 m long Cherenkov counters provide information for the electron separation. The muon content is about 5%, independent of the beam momentum. The momentum spread in the beam is about 1%. In the momentum range that has been scanned during those test measurements, the kinetic energy of electrons and pions is to a very good approximation equivalent to the beam momentum, thus for the sake of simplicity we will refer further to the beam energy instead of beam momentum.

2.2. DU calorimeter

The DU calorimeter consisted of five modules [3] with an effective lateral cross-section of 60×60 cm^2

0168-9002/91/$03.50

Table 1
Details of the uranium calorimeter modules

	Type of module	
	Old	New
Sensitive area	60×60 cm^2	60×60 cm^2
Number of DU–scintillator layers	30	45
Thickness of DU plates	3.2 mm	3.0 or 3.2 mm
Thickness of scintillator strips	5.0 mm	3.0 mm
Total thickness	390 mm $\approx 30X_0$ $\approx 1.1\lambda_{int}$	405 mm $\approx 44X_0$ $\approx 1.5\lambda_{int}$

each. Four of the five modules, the so called new modules were made of 45 uranium–scintillator layers adding up to 1.5 interaction length each. The uranium plates were 3 mm thick in three modules and 3.2 mm thick in the fourth one. The scintillator plates, 3 mm thick, consisted of 12 horizontal strips 50 mm wide. The fifth and last module was made of 30 layers, with each layer made out of 3.2 mm thick uranium plates and 5 mm thick scintillator strips. The total depth of this last module was equivalent to $1.1\lambda_{int}$. The light from the scintillator strips is collected at both ends over the full depth of each module through wavelength-shifter bars and guided to the photomultipliers. The signal from each photomultiplier is then digitized with a 12-bit LeCroy ADC (type 2282B). The calorimeter was installed on a vertical movable stand. The main characteristics of the DU calorimeter are summarized in table 1. The interested reader is referred to ref. [3] for more details.

2.3. The backing calorimeter

The prototype of the backing calorimeter (BAC for short) was made out of nine iron plates 88×96 cm^2, 5 cm thick, interleaved with ten layers of Iarocci-type limited streamer tubes (LST for short) [4], one in front of the first iron plate. The total thickness of the prototype was 65 cm, equivalent to $26X_0$ or $2.7\lambda_{int}$ (see table 2). A single tube consists of a plastic profile coated with graphite, containing eight square, 1×1 cm^2, cells, with a 100 μm wire stretched along the center of each. The profile is closed in a gas-tight box. 8.4 cm wide and 120 cm long. In order to operate in the limited streamer mode a mixture of 70% iso-C_4H_{10} + 30% Ar was used. The high voltage was set at 3.88 kV. One sensitive layer consisted of 12 such tubes, four adjacent ones forming one chamber. There were thus three chambers per layer, the so-called up, middle and down chambers. Signals from the wires within each chamber were summed together. The resulting chamber signals could be accessed one by one, giving the so-called chamber readout. In addition, the signals from the nine tube layers situated inside the iron calorimeter were summed, separately for the up, middle, and down chambers, in three horizontal towers, the so-called wire towers. On the outside, the chambers (except for the first layer) were equipped each with three square pads made of phenol plates covered with copper. The lateral structure of each layer consisted thus of nine pads (see fig. 1). The pad signals were summed in depth, in nine horizontal pad towers. All signals, after amplification, were digitized with a 12 bit ADC (the same as for DU calorimeter). Most of the data were taken with the BAC calorimeter standing behind the DU modules with no dead material in between. In order to match the geometrical structure of the ZEUS calorimeter, subsequent uranium modules were moved, and an energy scan of the combined calorimeters of different depths was performed. In order to study the performance of the stand alone BAC, the iron calorimeter was placed on the movable stand in front of the DU modules.

Table 2
Details of the test backing calorimeter

	Test backing calorimeter
Sensitive area	88×96 cm^2
Number of absorber layers	9
Thickness of absorber layers	5.0 cm
Total thickness	65 cm $\approx 26X_0$ $\approx 2.7\lambda_{int}$

3. Performance of the stand alone DU calorimeter

3.1. Calibration

The DU calorimeter was calibrated by two different procedures [3]. In one case, data from the lateral energy scan of each module by electrons have been used. In the other case, the natural radioactivity of the depleted uranium is used. In each case the uranium radioactivity – the so-called uranium noise – is used for monitoring the stability of the calorimeter response. The calibration constants are derived under the assumption that each photomultiplier should see the same signal. For the absolute calibration of the calorimeter, a slight correction has to be applied to one of the first four modules to take into account the difference in thickness of uranium plates. The fifth and last module needs altogether a different approach since it is equipped with 5 mm thick scintillator strips, as compared to 3 mm strips in the four modules. The absolute calibration of the DU

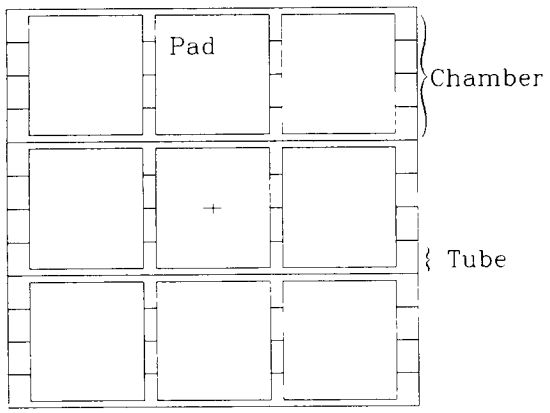

Fig. 1. Pad structure of the test backing calorimeter.

calorimeter for energy measurement of hadron showers will be discussed at length in one of the following chapters.

3.2. Response to electrons

A study of an energy scan of the first module of the DU calorimeter with electrons in the energy range of 10 to 50 GeV shows that the response is linear to within less than 1% [3]. A $\pm 3\sigma$ Gaussian fit to the observed energy distribution leads to an energy resolution $\sigma/E = 16.8\%/E^{1/2}$ with a constant term of 1.2% due mainly to the beam momentum spread.

3.3. Response to hadrons

The calorimeter response to hadrons has been studied for incident beam energies in the range of 10 to 100 GeV. The response was found to be linear to within less than 1%. No side-leakage correction was applied. The energy resolution has been studied after applying a stringent cut on the longitudinal leakage into the fifth uranium module. No shift of the central peak of the energy distribution was observed. A $\pm 3\sigma$ Gaussian fit to the energy distributions obtained for different energies with the longitudinal leakage cut leads to an energy resolution $\sigma/E = 35.7\%/E^{1/2} \pm 1.3\%$.

4. Performance of the stand-alone backing calorimeter

4.1. Calibration

The calibration of the BAC prototype was performed using 100 GeV muons directed at the center of each pad tower. A typical response to muons for one of the chambers is shown in fig. 2, after pedestal subtraction. The muon signal is seen as a second peak with a long Landau tail. The first peak is due to the inefficiency of the chambers with a width due to electronic's

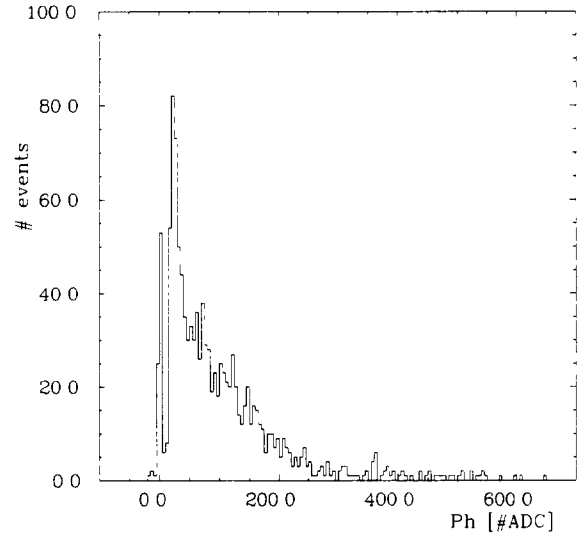

Fig. 2. Response of a single chamber to muons.

and chamber's noise. The efficiency of the chambers in the middle, where the wire supports are located, is significantly worse than on the sides. It is typically 90% at both ends and drops to 80% in the middle. For the relative calibration of the chambers only measurements on the side of the chambers were used, since the lateral spread of hadronic shower is such that the energy measurement is not sensitive to the position of wire supports. The mean pulse height is around 100 ADC channels for most of the chambers with a spread of about 30 ADC channels (see fig. 3), with the exception of two chambers with some damaged wires and one chamber with a noisy tube. The same procedure has

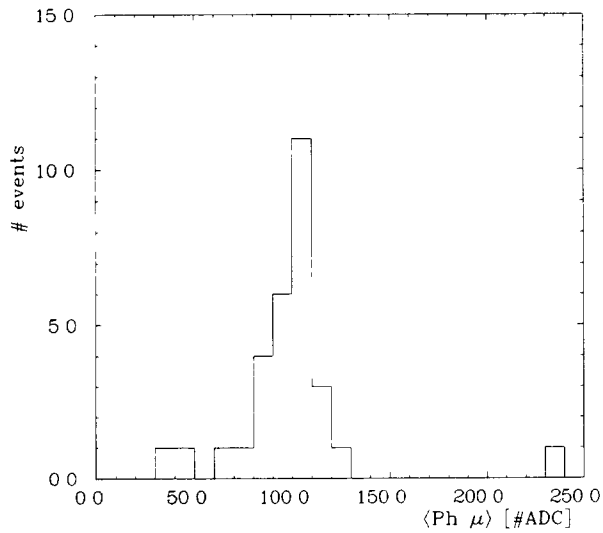

Fig. 3. Spread of calibration constants for all the chambers.

been applied to wire towers which are 100% efficient. The calibration of pad towers is more difficult, since there is a negative correlation between signals on adjacent pads situated along the same chamber. The correlation can contribute up to 10% of the total signal and depends strongly on the position of the beam. Thus a simple calibration by the mean muon pulse height does not guarantee a uniform response over the face of the detector. The data analysis has been carried out for the three methods of readout separately. The final response of the calorimeter is expressed in terms of the number of equivalent particles (nep, for short) after summing up all the channels of a given readout. After taking into account properly the number of active layers, the different readout methods are expected to give the same results.

4.2. Response to electrons

The electron response has been measured at 5, 10, 20 and 30 GeV. For electromagnetic showers, a large fraction of the energy can be deposited in a single layer. For higher beam energies ADC overflow effects were observed for the chamber readout. At 20 and 30 GeV, 36% and 75% of events had to be rejected, respectively. The ADC overflow effect is negligible for the pad electronics, while 10% of all events had to be rejected for 30 GeV electron showers for the wire tower readout. The calorimeter response for 20 GeV electron showers, as measured with the chamber readout, is shown in fig. 4 together with the result of a Gaussian fit. The dependence of the mean electron response as determined from the Gaussian fits on the beam energy, for the three different readout methods is shown in fig. 5. There is a clear deviation from linearity for the chamber and wire tower readout. The dependence of the pulse height on the incident energy is affected by the rejection of events with ADC overflows, as well as by saturation in the chamber, when several particles cross a tube within an area smaller than needed to initiate separate streamers. Saturation has been observed in the pad readout when

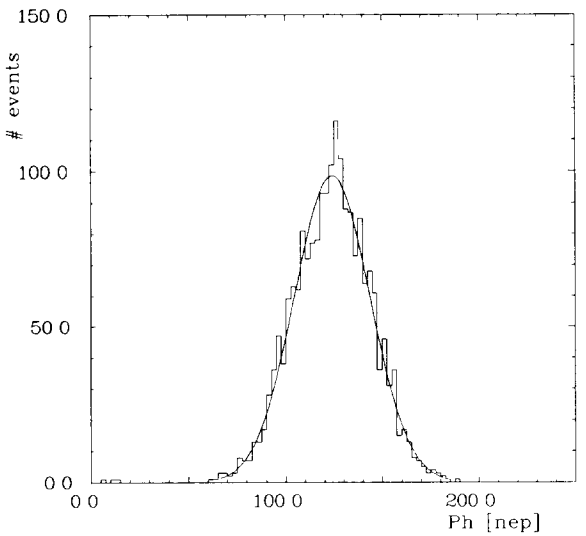

Fig. 4. Response of the BAC calorimeter (chamber readout) to 20 GeV electrons expressed in terms on the number of equivalent particles (nep). The curve is a Gaussian fit to the distribution performed within $\pm 3\sigma$.

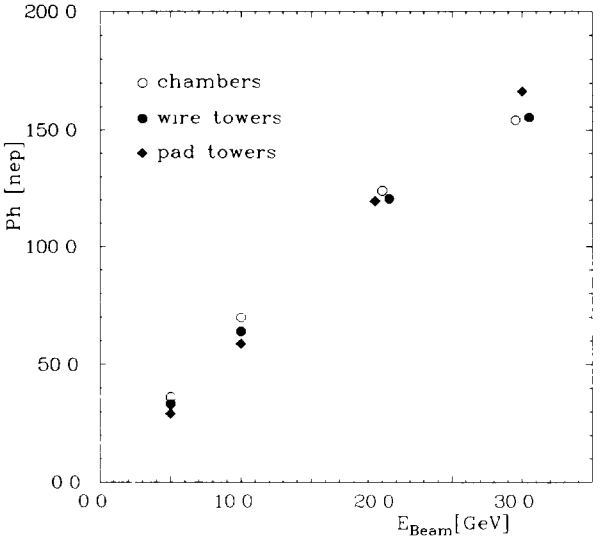

Fig. 5. The dependence of the mean electron pulse height on the beam energy, for chamber, wire-tower and pad-tower readout.

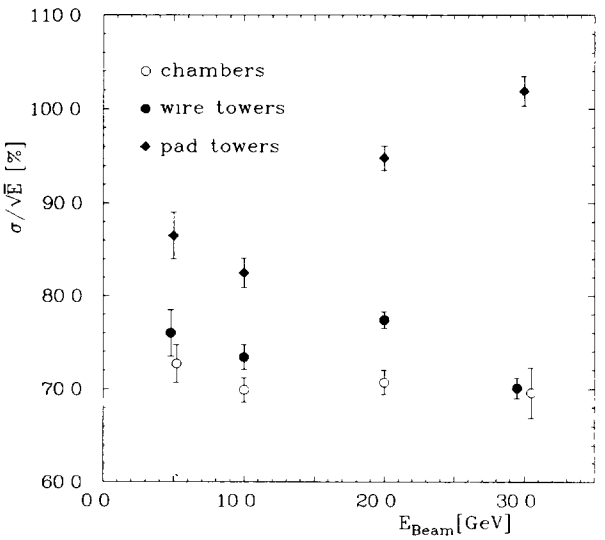

Fig. 6. The energy resolution of the BAC calorimeter for electromagnetic cascades, for chamber, wire-tower and pad-tower readout.

the signal is taken only from the pad tower hit by the electron beam. The much better linearity of the pad readout when summed over all towers (only a small deviation is observed at 30 GeV) can be understood as a fortuitous compensation of streamer saturation and pulses of the opposite charge induced in neighbouring pad towers. The energy resolution obtained from the Gaussian fits is shown in fig. 6. The chamber readout leads to an energy resolution $\sigma/E = 70\%/E^{1/2}$. The wire tower readout gives only a slightly lower resolution. However, the pad readout resolution worsens significantly with energy, which might well be due to the convolution of the effects mentioned above. The $70\%/E^{1/2}$ resolution is to be compared with $55\%/E^{1/2}$ obtained by the Aleph Collaboration [5] in similar condition. In our case we expect a worse resolution since the electron beam crosses the calorimeter close to the wire supports.

4 3. Response to hadrons

As the calorimeter is only $2.7\lambda_{int}$ deep it does not contain all hadron showers. Thus only low energy hadrons can be studied and cuts have to be applied to select a biased sample of events which tend to be dominated by the electromagnetic component and thus do not produce substantial leakage. Hadrons of 10, 20 and 30 GeV were studied. The ADC saturation problem is much less severe for hadrons, owing to the lateral spread of hadron showers. The hadron beam is contaminated by muons and electrons. This contamination has been rejected by studying the longitudinal structure

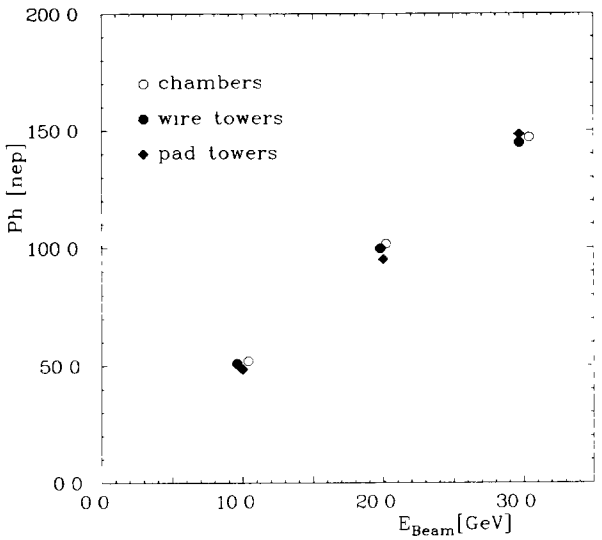

Fig. 8. The mean BAC calorimeter response to fully contained hadronic showers, as a function of the beam energy, for chamber, wire-tower and pad-tower readout.

of showers with the chamber readout. Electrons deposit most of their energy in the first four layers of the calorimeter, while muons are expected to deposit their energies uniformly along the calorimeter. In order to accept only showers fully contained in the iron calorimeter, a leakage cut was applied to the uranium module standing, in this particular configuration, behind the BAC calorimeter. All events with an energy deposition of more than 1% of the total beam energy in the

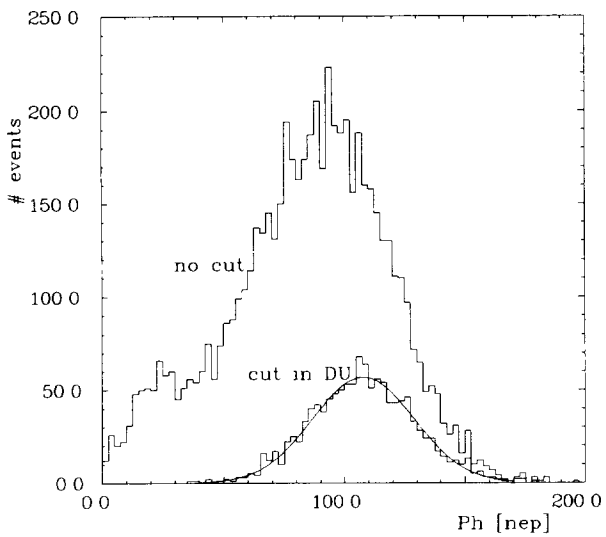

Fig. 7. Response distribution for 20 GeV hadron showers fully contained in the BAC calorimeter compared to the response distribution for all 20 GeV hadron events. The Gaussian curve fitted to fully contained hadron showers is also shown.

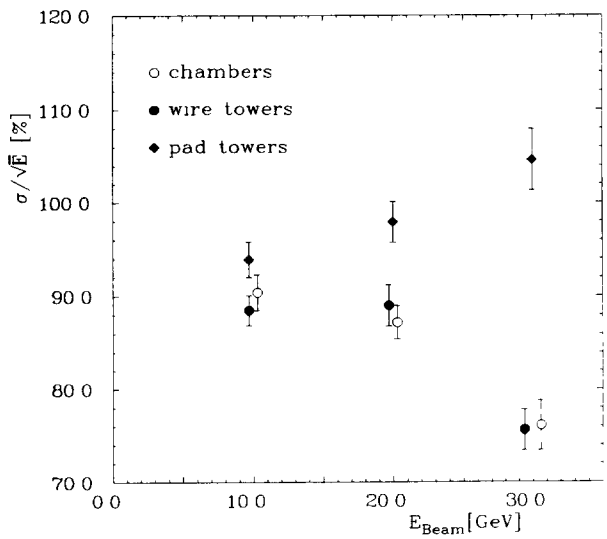

Fig. 9 The energy resolution of the BAC calorimeter for fully contained hadronic showers, for chamber, wire-tower and pad-tower readout.

uranium module were rejected. The total pulse height distributions measured for 20 GeV hadrons obtained with and without leakage cut are shown in fig. 7. Only 23% of events remained after the cut. Their pulse height distribution has been fitted with a Gaussian distribution that is shown in the same figure. The same procedure has been applied at the two remaining energies. The response of the calorimeter is linear with energy to within 3%, independent of the readout (see fig. 8). The resolution is around $90\%/E^{1/2}$ and improves with energy for chamber and tower readout (fig. 9). This is a direct consequence of the leakage cut, which tends to increase the percentage of events dominated by π^0 production with energy. The worsening of the pad readout resolution may be due to the lateral nonuniformity of the calorimeter response which affects stronger high energy showers than low energy showers. The $90\%/E^{1/2}$ resolution is to be compared with $84\%/E^{1/2}$ obtained by ALEPH Collaboration after applying a weighting procedure [5] and $100\%/E^{1/2}$ obtained by the H1 Collaboration with the same weighting procedure and 7.5 cm thick iron plates [6].

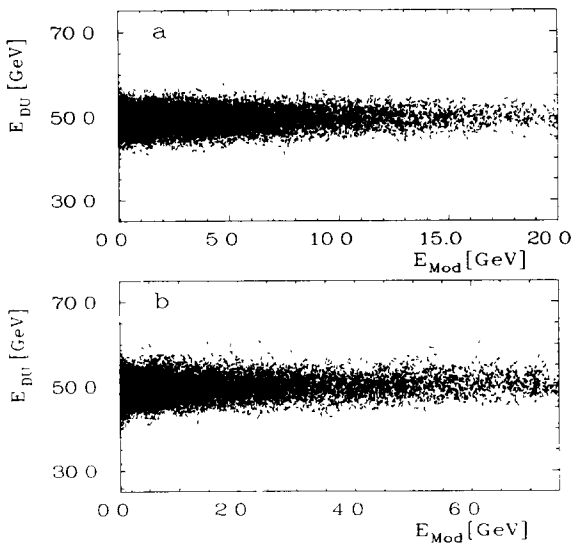

Fig. 10. The response of the DU calorimeter as a whole to 50 GeV, contained hadron showers, as a function of the energy deposited in the third module (a), and in the last, the so called "old" module (b) after the relative calibration of all the modules.

5. Combined DU and backing calorimeter

The performance of the combined DU and backing calorimeter was carried out for three different setups and three different hadron energies. The setups consisted of three, four or five uranium modules and the BAC calorimeter standing behind. The effective depth of the DU modules was of 4.1, 5.6 and $7.1\lambda_{int}$, respectively (corresponding to the forward, barrel and rear part of the ZEUS uranium calorimeter). Data was collected with a hadron trigger at energies of 30, 50 and 100 GeV. The total sample consisted of 450 000 events, with 80 000 events collected for three modules setup and 185 000 events for each of the two remaining ones.

5.1. Intercalibration

In order to understand the problem of intercalibration of two different calorimeters, the longitudinal shower development has been studied first in terms of the stand-alone calibration of both calorimeters. The absolute calibration of the BAC calorimeter is derived from the hadron energy scan reported in the previous chapter. The absolute energy calibration of the DU calorimeter is more difficult, since two out of the five modules have a different structure than the others. The relative calibration of the individual channels within each module was obtained by equalizing the uranium signal. The relative calibration between the modules was obtained from the condition that the total signal from all modules should be independent of the pulse height sharing between the modules. As an illustration, figs. 10a and 10b show scatter plots of the total signal E_{DU} versus the signal in an individual module, E_{mod}, for modules 3 and 5 after calibration. It has been checked that the relative calibration constants do not depend on

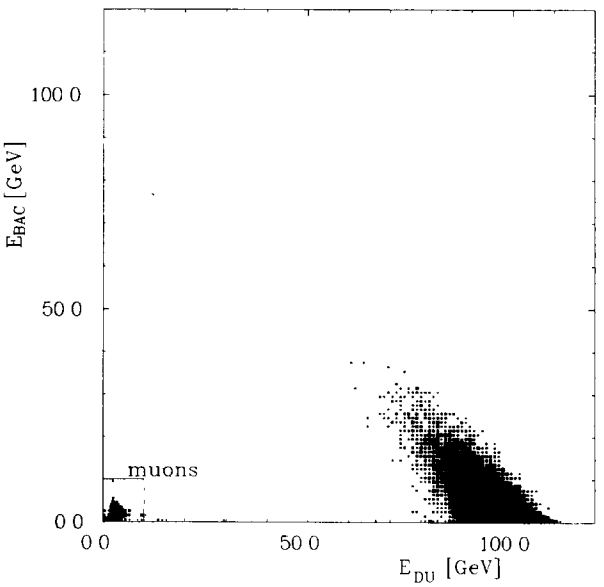

Fig. 11. Correlation between the energy deposited in the BAC calorimeter and the energy measured in the DU calorimeter, consisting of four modules, for a 100 GeV hadron beam. The contamination of the beam by muons is well visible. Also shown is the cut applied in order to reject muon events.

the setup and they do not depend on the incoming beam energy.

The correlation between the energy deposited in the DU calorimeter and the energy measured in the BAC calorimeter, for 100 GeV hadrons crossing 4 DU modules is presented in fig. 11. The contamination of muons is clearly observed. To suppress the longitudinal energy leakage out of the calorimeter system, a cut was applied in the last two chamber layers in the BAC calorimeter. The test backing calorimeter has a bigger sensitive area than the DU modules (see tables 1 and 2) and thus also monitors the energy leaking from uranium on the sides. The only area of the DU calorimeter that is not protected by the BAC calorimeter is the bottom of the calorimeter, where it is standing on concrete blocks. In order to suppress events with leakage in this region all

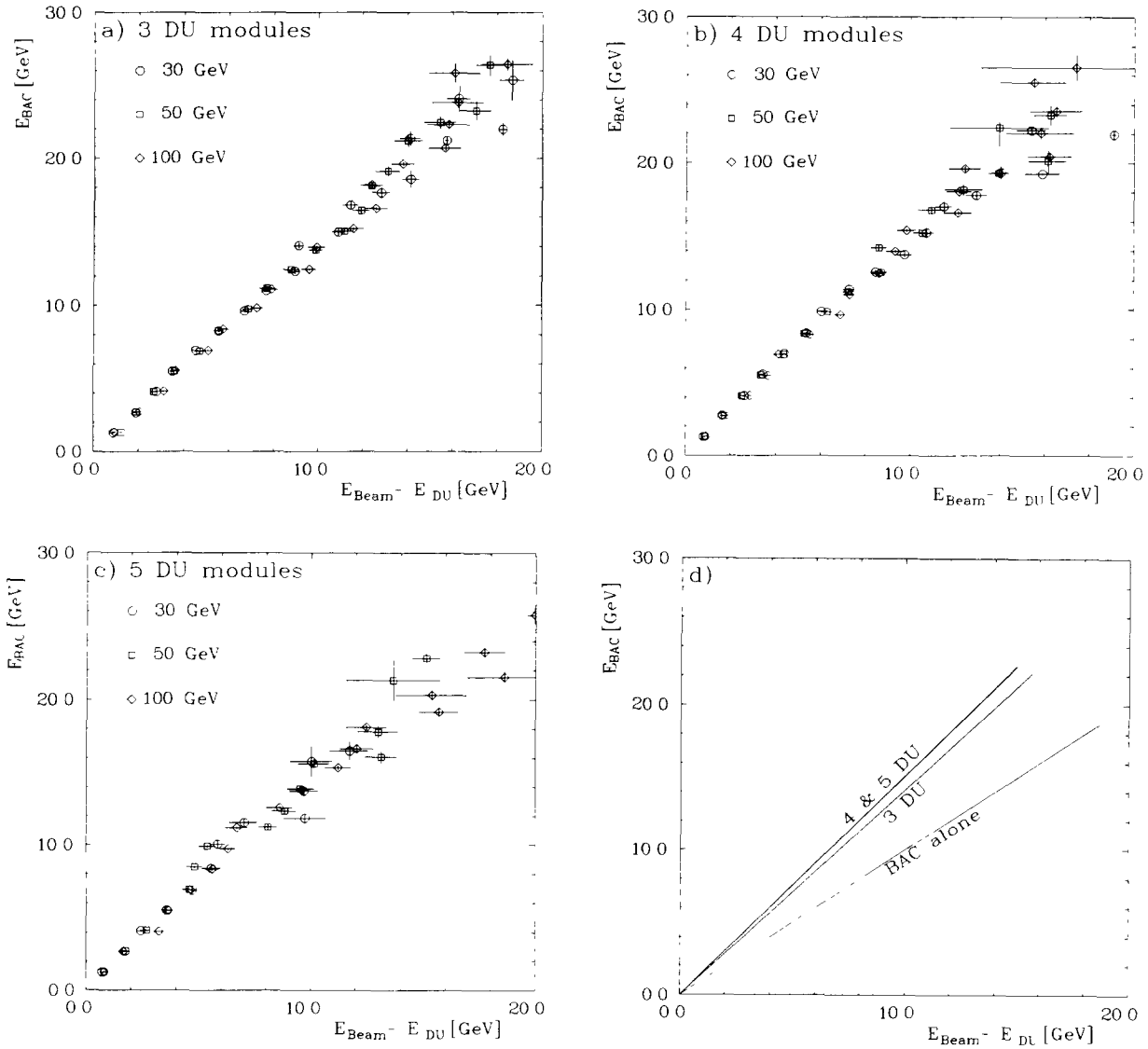

Fig. 12 (a) Mean response (in GeV) of the BAC calorimeter as a function of the energy missing in the DU calorimeter for 30, 50 and 100 GeV hadron showers with the DU calorimeter consisting of three modules (b) Mean response (in GeV) of the BAC calorimeter as a function of the energy missing in the DU calorimeter for 30, 50 and 100 GeV hadron showers with the DU calorimeter consisting of four modules. (c) Mean response (in GeV) of the BAC calorimeter as a function of the energy missing in the DU calorimeter for 30, 50 and 100 GeV hadron showers with the DU calorimeter consisting of five modules. (d) Mean response of the BAC calorimeter (in the form of the fitted lines) as a function of the energy missing in the DU calorimeter consisting of three, four and five modules, compared with the response determined from the stand-alone calibration of the BAC calorimeter

events with an energy deposit in the lowest three strips of the DU modules greater than 5% of the total energy are rejected.

5.2. Measurement of the energy leakage from the DU calorimeter

In order to study the response of the BAC calorimeter to showers leaking out of the DU calorimeter, the hadron events were divided into samples, according to the ratio of the energy measured in the BAC calorimeter, E_{BAC}, and the total energy $E_{DU} + E_{BAC}$ (this takes care of the inherent correlation between E_{BAC} and E_{DU}). The mean values of E_{BAC} and of the energy missing in the DU calorimeter $E_{Beam} - E_{DU}$ were then evaluated for every sample. The results, for different energies and different setups of the DU calorimeter, are presented in figs. 12a, 12b and 12c. It is seen that independently of the incident energy the response of the BAC calorimeter is proportional to the energy missing in the DU calorimeter. At high missing energies a slight deviation from linearity appears, which can be understood as due to energy leakages through the sides of the BAC.

For each of the configurations mentioned above, a linear dependence of the BAC response on the energy missing in uranium has been fitted. The results, in the form of the fitted lines, are compared with the response of the stand-alone BAC calorimeter in figs. 12a and 12d. The response of the calorimeter to hadronic showers leaking from uranium is higher than that to a single hadron of the same energy. A slight dependence on the layout is also observed. This change in the response of the BAC calorimeter may be due to many factors. Although the electromagnetic component in the leaking tail of the shower is expected to be suppressed, the contribution of the highly ionizing low energy particles may dominate, resulting in an overall increase of the signal. Part of the effect is due to the difference in resolution between the DU and BAC calorimeters. This has been checked by a simple Monte Carlo program which was based on a simple parametrization of the longitudinal shower development [7]. The BAC calorimeter response is sensitive to the distribution of deposited energy. The convolution of the calorimeter resolution with the steeply falling longitudinal profile results in an increase of the average energy measured in the BAC calorimeter. Another effect that may contribute to the increase of the signal in the BAC calorimeter for a given energy leaking out of uranium is due to the fact that hadronic showers developing in uranium contain a significant number of neutrons with energies in the MeV range. These neutrons can leak out from the DU modules. If so, they will penetrate into the BAC calorimeter, and may knock out low energy protons from the organic gas in the tubes, with a substantial hydrogen component. Thus neutrons may contribute to the effective compensation of the BAC calorimeter [8]. Also some of the neutrons leaking sideways from the DU calorimeter may be detected in the BAC calorimeter. The contribution of these neutrons which depends on the detector layout, may explain small differences in the BAC calorimeter response for different depth of the DU calorimeter. In conclusion, in order to measure the energy leaking out of three, four and five DU modules, the absolute calibration of the BAC calorimeter has to be decreased by factors of 1.41, 1.51 and 1.51 (± 0.04), respectively.

5.3. Impact of the backing calorimeter on total energy measurement

The influence of the BAC calorimeter on the hadron energy measurement in the test detector was studied for three, four and five DU modules standing in front of the BAC calorimeter, at 30, 50 and 100 GeV, respectively. These energies correspond to the maximum jet energy for a given depth of the uranium calorimeter in the ZEUS detector. In all those cases most of the events are well contained in the DU calorimeter, although there is still a significant tail of events with large energy deposits in the BAC calorimeter (see for example fig. 13a). This tail (on the low energy side) is also clearly visible in the response distribution of the DU calorimeter, when no cut on longitudinal energy leakage is applied (fig. 13b). To preserve better energy resolution, the BAC calorimeter has to be used to reject these events or to correct the measurement by adding the leaking energy. In both cases the shape of the measured energy distribution improves significantly as compared to the noncorrected spectrum (see figs. 13c and 13d).

One of the problems in describing the properties of the energy distribution obtained by adding the response of two different calorimeters is that the final distributions tend to develop non-Gaussian tails. In order to describe the distributions under consideration two different estimates were chosen:

- The width of the distribution is estimated through the rms of the distribution truncated to the range of $\pm 3\sigma$ around the maximum, where σ is determined from FWHM and the position of the maximum with a Gaussian fit, applied in the region above $\frac{2}{3}$ of the value at the maximum;
- Its "skewness" is estimated through the fraction of events below 3σ from the maximum.

This approach has been applied to all distributions, those obtained for the response of the DU calorimeter after rejecting events in which the signal observed in the BAC calorimeter was above a certain fraction of the beam energy, as well as those obtained after rejecting the same events, but adding the energy measured in the

BAC calorimeter to that measured in uranium. The dependent of the resolution, calculated from the estimated width, and of the fraction of events in the low energy tail on the cut applied in the BAC calorimeter, for the DU calorimeter consisting of four modules, exposed to a beam of 50 GeV hadrons are presented in fig. 14. The rejection of events with significant energy deposits in the BAC calorimeter improves the energy resolution of the DU calorimeter from about $41\%/E^{1/2}$ (with no cut) to $36\%/E^{1/2}$ (for 1% cut) while the fraction of events in the low energy tail (large missing energy) decreases by over an order of magnitude, that is from $(7.6 \pm 0.2)\%$ to $(0.5 \pm 0.1)\%$. A significant improvement of the energy resolution of the stand-alone DU calorimeter is also observed when the signal from the BAC calorimeter is used to correct the energy measured in the DU calorimeter. The influence of the BAC calorimeter stops to be important when the missing energy is below 3% of the total energy. The same remains true for the other two configurations of the DU modules. The results for the resolution of the DU calorimeter, as a function of the cut on the fractional energy leakage into the BAC calorimeter, are summarized in table 3.

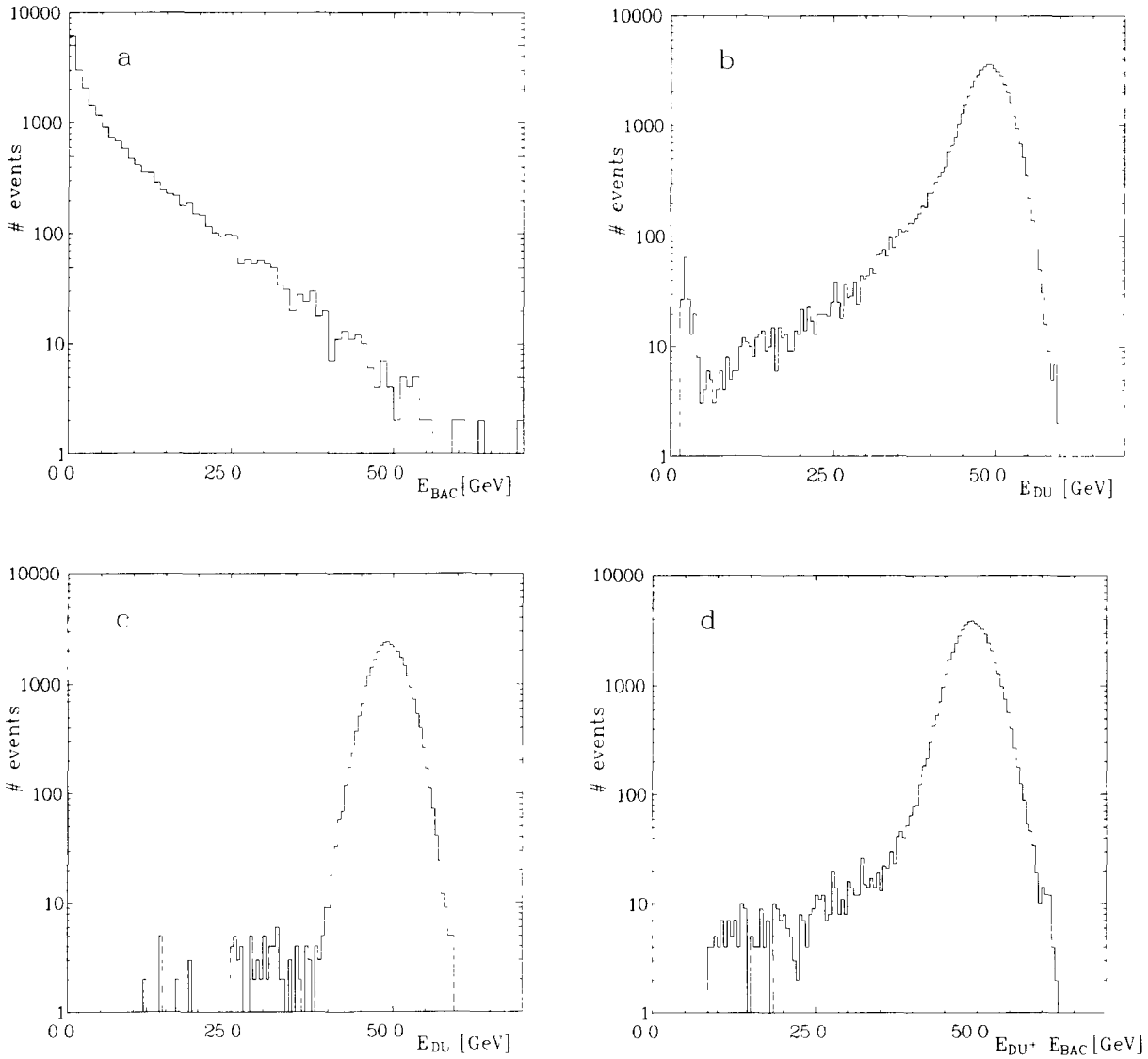

Fig. 13. Distribution of the energy measured in the BAC calorimeter (a), in the DU calorimeter (b), in the DU calorimeter after applying a 1% cut on the fractional energy leaking into the BAC calorimeter (c), and in the combined DU and BAC calorimeters (d), for the DU calorimeter consisting of four modules and 50 GeV hadron showers.

Table 3
The energy resolution $\sigma/E^{1/2}$ for the DU calorimeter alone, and the fraction of events f_{ev} remaining after the cut, as a function of the cut on the fractional energy leakage into the BAC calorimeter C_{BAC}, for different configurations of the DU calorimeter

C_{BAC} [%]	Configuration					
	3 DU modules 30 GeV		4 DU modules 50 GeV		5 DU modules 100 GeV	
	f_{ev} [%]	$\sigma/E^{1/2}$ [%]	f_{ev} [%]	$\sigma/E^{1/2}$ [%]	f_{ev} [%]	$\sigma/E^{1/2}$ [%]
No cut	100	46.3	100	41 3	100	43.7
20	86	44.6	96	41.1	99	43.7
15	83	43.2	94	40.6	98	43.7
10	78	41.5	90	39.3	96	43 1
8	75	40.7	88	38.6	95	42.5
5	70	39.3	84	37.5	92	41.1
3	65	38.4	79	36.7	88	40.3
1	58	37.7	70	36.0	79	39.5

5.4. The influence of a nonactive layer on the energy measurement

In the test setup the BAC calorimeter was placed right next to the DU calorimeter. In the original design of the ZEUS detector the backing calorimeter is separated from the uranium calorimeter by a nonactive layer consisting of the mechanical supports, a layer of photomultipliers and their shieldings, part of the electronics and cables. The nonactive layer is estimated to be equivalent to about 10 cm of iron. To study the influence of this dead material on the energy measurement in the detector, a nonactive area has been simulated in the test detector by ignoring in the analysis selected tube layers of the BAC calorimeter. By omitting signals from consecutive chambers a nonactive layer of 5 up to 25 cm of iron could be simulated.

The influence of different thickness of a nonactive layer on the energy measurement was studied for the uranium prototype consisting of four modules and for beam energy of 50 GeV. In every case the whole analysis was repeated exactly as described in the previous section. First of all the calibration of the BAC calorimeter has to be reevaluated due to the energy losses in the dead region. Fig. 15 shows the dependence of the mean response of the BAC calorimeter on the energy missing in the DU calorimeter, for different thickness of the nonactive layer. Though the energy losses in the nonactive layer can be large, the mean response of the BAC calorimeter remains proportional to the energy leaking out of the DU calorimeter. This implies that the energy lost in the dead layer is strongly correlated with that measured in the BAC calorimeter. It is thus possible to correct on average for this losses by changing appropriately the calibration factor for the BAC calorimeter, which comes out to depend linearly on the iron thickness.

This factor, however, is evaluated by considering the mean signals only. It is clear that on an event by event basis the fluctuations in the shower development will affect the measurement of the energy leaking from the

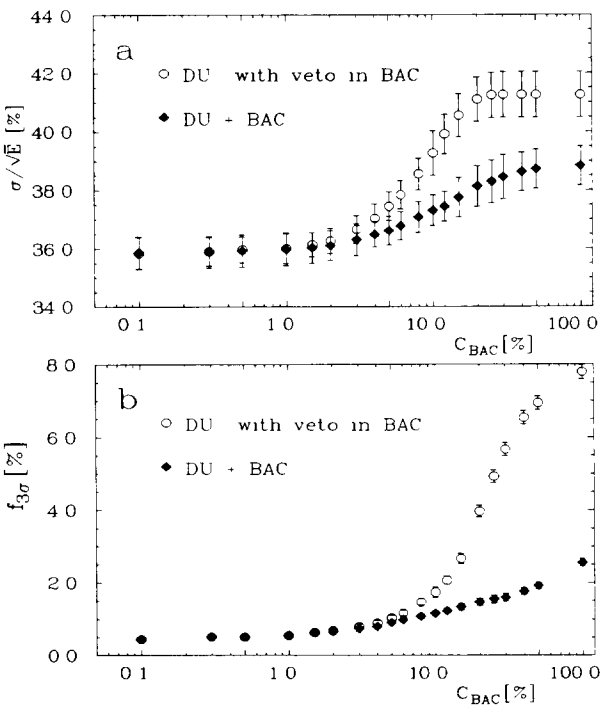

Fig. 14. The influence of the cut on the fractional energy leakage into the BAC calorimeter C_{BAC} on the energy resolution $\sigma/E^{1/2}$ (determined from the rms of the distribution contained in $\pm 3\sigma$ around the maximum) (a), and on the fraction of events with energy deposits below 3σ from maximum $f_{3\sigma}$ (b) for the DU calorimeter alone and the combined DU and BAC calorimeters, for a 50 GeV hadron beam and four DU modules.

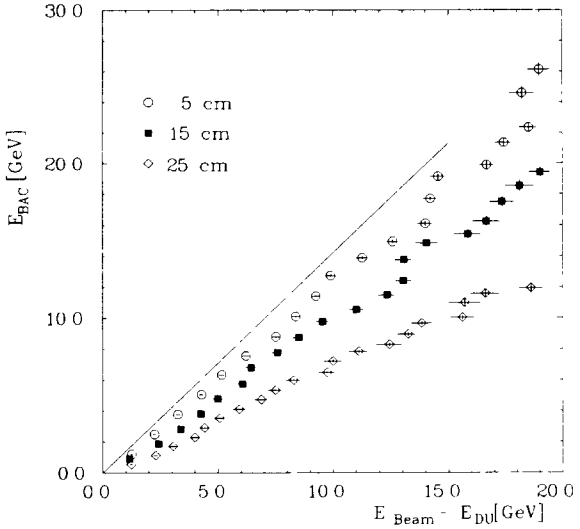

Fig. 15. Dependence of the mean response of the BAC calorimeter on the energy missing in the DU calorimeter consisting of four modules, for different thickness of the nonactive iron layer in front of the BAC calorimeter d_{Fe}, for 50 GeV hadrons. Also shown is the response of the BAC calorimeter with no iron layer in front.

DU calorimeter. Fig. 16 shows the distribution of the energy lost in a nonactive layer of 15 cm for events which gave a signal of less than 1% of the beam energy in the remaining activity part of the BAC calorimeter. For about 11% of those events the lost energy is greater

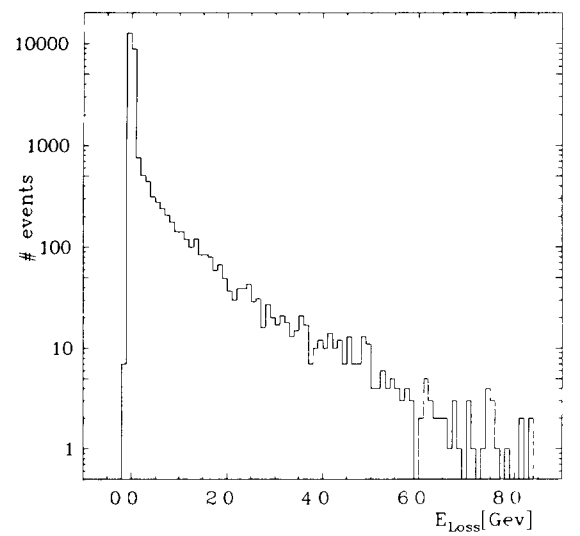

Fig. 16. Distribution of the energy losses in a nonactive layer consisting of 15 cm of iron located behind the DU calorimeter consisting of four modules, for 50 GeV hadron showers, after a 1% cut on the energy leakage into the BAC calorimeter has been applied.

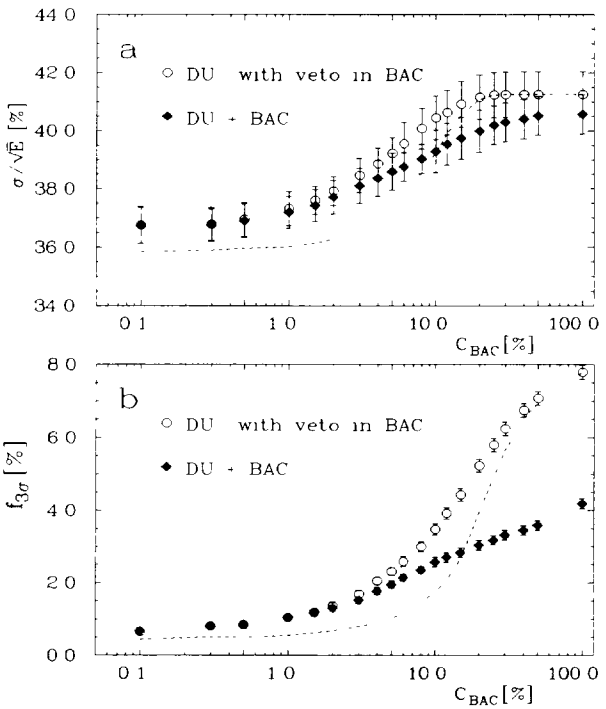

Fig. 17 The influence of the cut on the fractional energy leakage into the BAC calorimeter C_{BAC} on the energy resolution $\sigma/E^{1/2}$ (a) and on the fraction of events with energy deposits below 3σ from maximum $f_{3\sigma}$ (b) for the DU calorimeter consisting of 4 modules and for the combined DU and BAC calorimeters, for a 50 GeV hadrons and a nonactive layer of 20 cm of iron. The dashed line denotes the dependence determined with no nonactive layer between the two calorimeters.

than 1% of the incident energy. However, the tail of the distribution drops very fast with the deposited energy, and only in about 0.3% of events the leakage is greater than 10% of the beam energy (to be compared with about 10% of events, had the information from the BAC calorimeter been ignored altogether). It is thus clear, that even in the case of a layer of a nonactive material the information from the BAC calorimeter is of interest.

The results on the energy resolution and a fraction of events in the low energy tail, for a nonactive layer of 20 cm are shown in fig. 17, as a function of the cut in the BAC calorimeter. For comparison the results for the DU calorimeter response without a dead area between are also included. The response of the DU calorimeter with a strong cut in the BAC calorimeter is only slightly affected by the presence of the nonactive layer. The effect of the cut on the energy leaking into the active part of the BAC calorimeter is comparable in size to the case without the nonactive region. The influence of the thickness of a nonactive layer on the resolution of the DU calorimeter and on the fraction of events contained

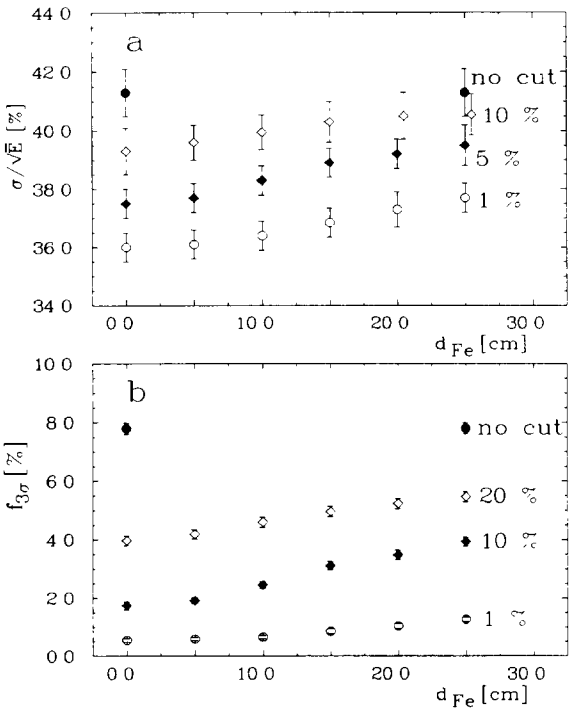

Fig. 18. Dependence of the energy resolution for 50 GeV hadrons, for the DU calorimeter consisting of four modules $\sigma/E^{1/2}$ (a), and of the fraction of events with energy deposits in the DU calorimeter below 3σ from maximum $f_{3\sigma}$ (b) on the thickness of the nonactive iron layer between the DU and BAC calorimeters d_{Fe}, for different values of the cut C_{BAC} on the fractional energy leakage into the BAC calorimeter.

in the low energy tail, for various cuts applied on the signal in the BAC calorimeter, is presented in fig. 18. Even in the presence of a nonactive layer up to 25 cm the BAC calorimeter works well as a veto for the energy leaking out of uranium. The improvement of the energy resolution by adding the energy deposited in the BAC calorimeter is less pronounced than in the case without the dead material.

It is clear that in order to achieve a substantial improvement in the resolution of the energy measurement for all events, the nonactive layer between the uranium calorimeter and the backing calorimeter should be as small as possible. If the thickness exceeds 10 cm equivalent of iron the improvement in the energy resolution will no longer be significant. The efficiency for correcting large energy losses also decreases fast with the thickness of the nonactive layer.

6. Conclusions

We have studied the performance of two combined calorimeters consisting of a prototype of the fine grain, high resolution uranium–scintillator calorimeter of the ZEUS detector followed by a much coarser backing calorimeter, made out of thick iron plates interleaved with planes of limited streamer tubes as an active material. The role of the backing calorimeter is to monitor the energy leakage from the uranium calorimeter, whose design was such as to ensure a 95% energy containment for 90% of the jets [9]. The test results, obtained in an exposure of the two calorimeters to a hadron test beam at the CERN-SPS, show that indeed the backing calorimeter gives a very efficient veto on the energy leaking out of uranium, thus improving substantially the energy resolution. Moreover, in spite of its resolution of $90\%/E^{1/2}$ as compared to $36\%/E^{1/2}$ of the uranium calorimeter it can be used to correct for the energy leakage, and still improves the resolution of the energy measurement. It can also be used to suppress events with large missing energy leaking out of uranium. It is of special importance in the search for events with large missing energy, which are a signal for many exotic processes expected in ep collisions at HERA energies. Even if the two calorimeters are separated by a nonactive layer of 5 to 25 cm equivalent of Fe, it is still possible to monitor the energy leakage from the uranium calorimeter and thus reject events with high energy leakage and preserve the high energy resolution of the uranium calorimeter. The fact that the backing calorimeter can be used either as a veto calorimeter or to correct for the energy leakage, allows a selection of samples with various energy resolutions depending on the purpose of the analysis.

The tests described in this paper were the first ones with a setup similar to the calorimeter structure proposed for the ZEUS detector. The results show that the idea of instrumenting the iron yoke of the detector with gas tubes to obtain a relatively low resolution hadron calorimeter surrounding the high resolution uranium–scintillator one works well in practice. The final backing calorimeter will differ significantly from the prototype described here, and thus further tests are needed. However, we have already good reasons to believe that with the calorimeter system of the ZEUS detector one will indeed be able to achieve a precise hadron energy measurement with full hermeticity.

Acknowledgements

We would like to thank the members of the ZEUS Collaboration, in particular our colleagues from the Calorimeter and the Barrel Muon groups, for their help and support in building our test setup at CERN, and for many useful discussions. Special thanks are due to G. Drews and F. Selonke for providing the on-line data acquisition system. We appreciate the hospitality and excellent technical support we have received at CERN,

where the measurements have been performed. This work would have not been possible without the financial support of the DESY Directorium.

References

[1] ZEUS, a Detector for HERA, Letter of Intent, DESY (June 1985);
The ZEUS Detector, Technical Proposal, DESY (March 1986);
The ZEUS Detector, Status rep. 1989, DESY (March 1989).
[2] Technical Proposal for the H1 Detector, DESY (1986);
Technical Progress rep., H1 Detector, DESY (1987).
[3] G. d'Agostini et al., Nucl. Instr and Meth. A274 (1989) 134.
[4] E. Iarocci, Nucl. Instr. and Meth. 257 (1983) 30.
[5] M.G. Catanesi et al., Nucl. Instr. and Meth. A247 (1986) 438.
[6] W. Braunschweig et al., Nucl. Instr. and Meth. A270 (1988) 334.
[7] R.K. Bock et al., Nucl. Instr. and Meth. 186 (1981) 533.
[8] W. Carithers, LBL/CDF Note 87-05;
C. Haber and J. Siegrist, LBL/CDF Note 87-08.
[9] J. Krüger, ZEUS Note 86-019, DESY (1986).